Fuel 405 (2026) 136476

Contents lists available at ScienceDirect

Fuel

journal homepage: www.elsevier.com/locate/fuel

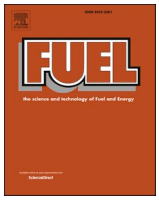

Full Length Article

Optically transparent solid-fuel to couple energy to the regression front

Yuxin Zhou, Lei Yang, Keren Shi, Michael R Zachariah *

University of California, Riverside, CA 92521, United States

ARTICLE INFO

Keywords:
Optical fiber
Laser heating
Solid fuel
Regression rate manipulation

ABSTRACT

A novel method to manipulate the regression rate of hydroxyl-terminated polybutadiene (HTPB) solid fuel through coupling light energy to the regression front, is demonstrated. A polymethylmethacrylate (PMMA) light pipe is pre-embedded in the solid fuel, with one end acting as the input port for laser light and another end located at the top-surface of solid fuel. Both HTPB and PMMA are de facto polymer fuels, therefore during the combustion, the light pipe regresses simultaneously with the regression front of HTPB fuel. As a result, radiation energy can be efficiently and conveniently coupled to the regression front, without the need for light input from the combustion side. Experimental results show that the regression rate of HTPB increases linearly with laser intensity, enabling for these conditions, up to a $\sim 1.72\times$ increase in output combustion power. The temperature of the regression front from IR measurement appears to be independent of laser energy. A one-dimensional energy-balance model shows that the energy penalty of using a laser is less than 2 %. This is because the majority of heat from combustion is convected away from the regression front, while laser energy is delivered to the reaction/regression front. Doping with graphine improves this strategy owing to its excellent laser absorption ability.

Both experimental and computational results indicate that the dependency of regression rate on laser energy density is close to linear, offering a good strategy to manipulate regression rate.

1. Introduction

Regression rate, the speed at which the front of solid fuel recedes, is a key metric in heterogeneous combustion, governing the overall energy release rate [1]. The manipulation of regression rate can be achieved through adjusting fuel/oxidizer component [2,3], doping metal particles [4,5], or controlling heat feedback by using additives [6–8]. An alternative approach is to add electromagnetic energy. For example, microwave energy can be uniformly deposited into the condensed phase of composites to form localized hot spots or into the gas phase combustion region of solid propellant to form a plasma by inelastic electron-neutral collisions [9–11]. There are also quite a few previous studies on the manipulation of solid fuel regression rate through the heat delivered using optical frequencies. Kakami et al. [12] delivered laser energy to the surface of non-self-combustible solid propellant and achieved a controllable combustion over a wide pressure range. Duan et al. [13] also employed laser irradiation to the surface of a propellant as an additional heat source and found that regression rate increased with laser fluence, while the thickness of thermal gradient beneath the regression front decreased. Similarly, Esker et al. [14] showed a positive correlation between solid fuel regression rate and laser fluence. Beyond the manipulation of regression rate, laser-assisted ignition has been explored for application as spatially-resolved igniters [15,16].

While it has been demonstrated that laser energy can manipulate the output combustion power, the actually delivery of energy from a laser source has always been problematic and not necessarily practically feasible. The usual approach is to propagate the light normal to the burning surface, but this necessitates optics that are stationed down-stream of the combustion, and the light must be propagated through the combustion product gas and particles. In contrast, if one could deliver energy from the up-stream one could avoid placing optics in the down-stream region of the combustion, where hot gases and combustion byproducts create addition complexities. In addition, particles in the combustion products can cause significant laser scattering, further reducing effectiveness and stability.

In this paper, we propose a novel method to deliver energy to the regression front from the up-stream, by directly transmitting the energy through the fuel grain. The basic premise is if the fuel is optically transmissive to light right up to the regression front, energy can be deposited there efficiently, without the need for the optical setup at

* Corresponding author.
E-mail address: mrz@engr.ucr.edu (M.R. Zachariah).

https://doi.org/10.1016/j.fuel.2025.136476
Received 27 April 2025; Received in revised form 16 July 2025; Accepted 5 August 2025
Available online 20 August 2025

down-stream of the combustion.

For this demonstration we embed polymethylmethacrylate (PMMA) which can act as both a light pipe and a fuel, within hydroxyl-terminated polybutadiene (HTPB), a widely-used de facto polymer fuel [5,17,18]. In air-breathing combustion, HTPB would first undergo two-stage decomposition (crosslinking and then breakdown), and finally release combustible gaseous species [19–21].

The key concept in this strategy is that PMMA, which can also be used as a de facto polymer fuel [22,23], is consumed at the regression front and regresses at the same rate as the surrounding HTPB. As such the terminus of the energy delivery is always at the regression front. This guarantees the continuous and precise coupling of the location of laser energy input and the regression front.

2. Experimental setup

2.1. Fuel fabrication

HTPB is mixed with methylene diphenyl diisocyanate (MDI) as a curing agent and isodecyl pelargonate (IDP) as plasticizer with a high-speed mixer (Thinky Ar-100) operating at 2000 rpm for 3 min. The mass fractions of HTPB, MDI and IDP are 78.4 %, 11.6 %, and 10 % respectively, a formulation that has been employed in our previous study [6]. The resulting mixture is poured into a 1 mL cylindrical container and allowed to cure at room temperature. The diameter of the final product is ~ 5 mm.

After the curing of HTPB, a PMMA optical fiber (diameter ~ 1 mm) is inserted into the center of the HTPB cylinder. The effects of additives on laser energy absorption are also examined. HTPB doped with graphite flakes (~325 mesh), as well as aluminum (Al) nanoparticles (nominal average diameter ~ 100 nm) are fabricated as well. Graphite flakes are attractive because of their excellent laser absorption efficiency, while Al nanoparticles are studied since they offer improved energy density and have been widely used as additives in various propellant formulations [5,6,24]. The fabrication method of HTPB doped with graphite flakes or Al nanoparticles is almost identical to that of HTPB. The only difference is that after the mixing of HTPB, MDI and IDP, the mixture is further blended with graphite flakes or Al nanoparticles using the high-speed mixer at 2000 rpm for an additional 3 min to ensure uniform dispersion of the additive.

HTPB, MDI and IDP are all purchased from RCS. Bare PMMA optical fibers are purchased from FiberFin. Graphite flakes are purchased from Alfa Aesar. Al nanoparticles are purchased from US Research Nanomaterials.

2.2. Experimental system

Fig. 1(a) illustrates our experimental setup. The HTPB fuel with the PMMA light pipe is oriented vertically on a stainless-steel holder. The length of the fuel grain is 1 – 1.5 cm. Fig. 1(b) shows the representative top-view SEM image of the embedded optical fiber. A continuous wave (CW) laser (532 nm, CivilLaser LSR532N-5 W) is employed as the source and the emitted laser is focused with a 100 mm FL convex lens, to the entrance of optical fiber. The input laser energy can be adjusted by the working current of the laser source; while both the laser energies before the entrance of optical fiber and at the exit of the HTPB fuel are measured by laser power meters (MKS Ophir), as shown by Power Meter − 1 and Power Meter − 2 in Fig. 1(a) respectively. In our configuration the initial input power density is varied up to 22.7 W/cm^2, with a transmission efficiency through the fuel as measured by Power Meter − 2 of ~ 60 % as shown by Fig. 1 (c). This loss is attributed to the fiber-laser coupling loss and the light reflection at the entrance of fiber. As depicted in Fig. 1(d), when energy is delivered to the regression front, a portion of the laser energy is absorbed, serving as an additional source of heat. Meanwhile, another portion penetrates the regression front and continues to propagate upward, representing an energy loss. Although the formation of char during the combustion is generally undesirable, in this strategy it plays a beneficial role. The presence of char within the regression front enhances the absorption of laser energy, thereby reducing the transmission loss and improving thermal coupling.

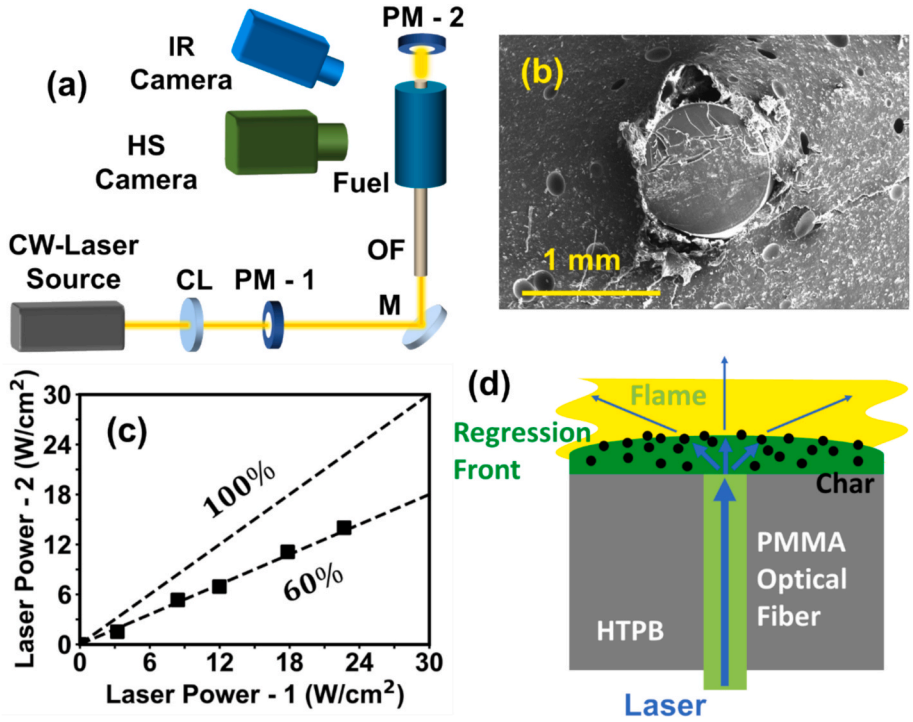

Fig. 1. (a) Experimental setup (CL: convex lens, PM: power meter, M: mirror, OF: optical fiber, IR: infrared, HS: high speed); (b) SEM image of pre-embedded PMMA optical fiber in HTPB; (c) Respective laser powers at the entrance and the exit of optical fiber; (d) Diagram of laser-coupled HTPB regression front during the combustion.

A high-speed camera (Phantom Vision Research Miro M110) operating at 200 fps is utilized to measure the regression rate of HTPB fuel. The view of the high-speed camera is perpendicular to the propagation of the HTPB fuel. Fig. 2 presents snapshots of the burning HTPB fuel at 6-second intervals. The regression of the surface is shown in the snapshots as the dashed yellow line in Fig. 2, which indicates a nearly linear regression of the fuel.

An infrared camera (Telops Fast M3K) is utilized to measure the surface temperature of HTPB fuel during combustion. The view of the IR camera is situated above the fuel grain at ~ 45° angle. An assumption of emissivity = 1.0 is employed in the IR measurements.

It should be noted that although two different polymer fuels have nominally different characteristic regression rates, the composite fuel (HTPB and PMMA optical fiber) burns as essentially a single component system from our observations, as presented in Fig. 2.

3. One-Dimension energy balance model

A quasi-one-dimensional model modified from the work of Kakami et al. [12,25] is implemented to help understand the influence of laser energy on the combustion of HTPB. The combustion of PMMA is ignored in this simplified model since the mass fraction of PMMA in the composite fuel is only ~ 5 %. The combustion of HTPB can be divided into three regions: (1) flame above the surface of HTPB where small hydrocarbon molecules (mainly C_4H_6) [3] released from the decomposition of HTPB react with oxidizer; (2) "liquid-like" regression front on the surface of HTPB where HTPB decomposes; (3) unburned zone beneath the surface of HTPB where pre-heating occurs.

Fig. 3 shows the relevant energy fluxes related to the regression front. $H_{F,1}$ is the heat feedback from the flame to the regression front. $H_{F,2}$ is the heat feedback from the regression front to the unburned zone. I_L is the laser energy flux delivered to the regression front, which is determined, as shown in Fig. 1(a). Q_d is the enthalpy change for HTPB decomposition.

Given this is a diffusion flame (air-breathing system) in our nomenclature we regard the "regression front" as sitting below the flame and is thus oxygen-deficient, and the main process at the front should be the pyrolysis of HTPB (i.e., the decomposition zone of HTPB). Therefore, the current model can further specify Q_d in the regression front. According to previous thermogravimetric analysis/differential scanning calorimetry (TGA/DSC) experiments of cured HTPB [26,27], the thermal decomposition of HTPB typically has two isolated DSC peaks, interpreted by an exothermic cross-linking and cyclization process below 400 °C, and an endothermic depolymerization process at ~ 450 °C. We can assume that these two sub processes all occur within the regression front, and thus the global enthalpy change during the decomposition, including both exothermic and endothermic steps, is estimated as $Q_d \sim -0.5$ kJ/g according to the baseline-removed integral of DSC peaks [26,27].

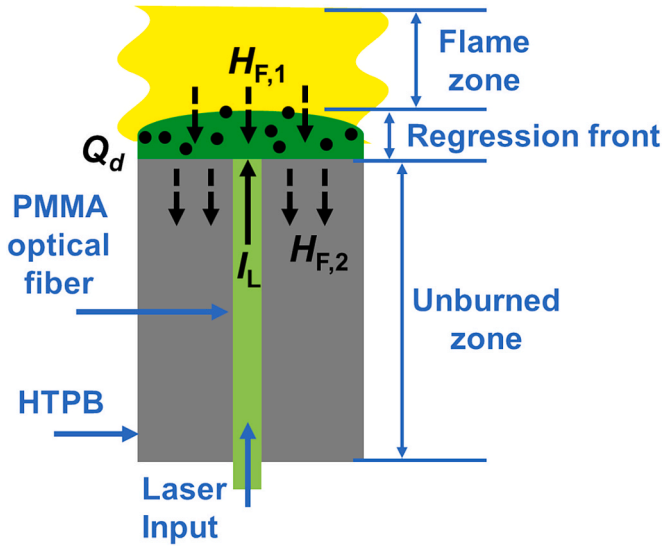

Fig. 3. Energy balance model.

Although the flame heat generation is not included in the current model, the contribution of combustion to the regression rate is accounted for through the heat feedback term $H_{F,1}$.

The energy balance of the regression front can be described by Eq. (1). Since not all the laser energy is absorbed, we employ an absorption efficiency η in Eq. (1).

$$H_{F,1} + \eta I_L = H_{F,2} + Q_d r \rho_{HTPB} \quad (1)$$

Where r is the regression rate; ρ_{HTPB} is the density of HTPB.

Based on one-dimensional heat conduction assumption, the heat feedback from the regression front to the unburned zone can be expressed by:

$$H_{F,2} = \rho_{HTPB} c_{p,HTPB} r (T_r - T_0) \quad (2)$$

Where T_r is the temperature of regression front; T_0 is ambient temperture.

Therefore, the dependency of regression rate, r, on the laser energy density can be expressed as:

$$r = a\eta I_L + b \quad (3)$$

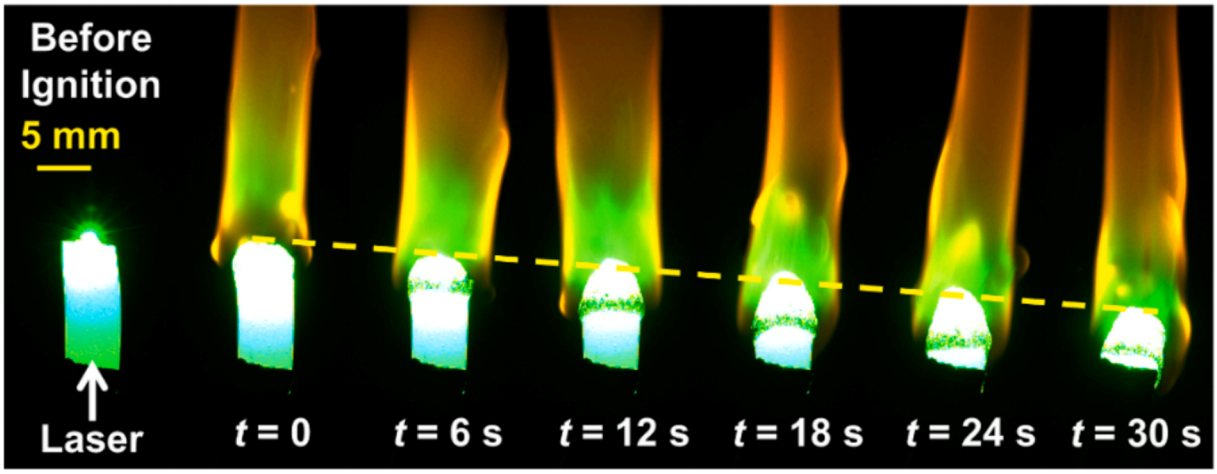

Fig. 2. Snapshots of the combustion process of HTPB fuel with laser energy input.

$$a = \frac{1}{\rho_{\mathrm{HTPB}} c_{\mathrm{p,HTPB}} (T_r - T_0) + Q_d \rho_{\mathrm{HTPB}}} \tag{4}$$

$$b = \frac{H_{\mathrm{F,1}}}{\rho_{\mathrm{HTPB}} c_{\mathrm{p,HTPB}} (T_r - T_0) + Q_d \rho_{\mathrm{HTPB}}} \tag{5}$$

Since the heat feedback from the flame to the regression front ($H_{\mathrm{F,1}}$) is difficult to measure, the regression rate when laser is turned off ($I_{\mathrm{L}} = 0$) can be used to determine b. More details in energy balance analysis can be found in previous studies by Kakami et al. [12,25].

The density of our HTPB fuel ρ_{HTPB} is measured experimentally (~ 880 kg/m^3), and is slightly lower than the typical value (~ 900 kg/m^3) [28]. Specific heat capacity of HTPB $c_{\mathrm{p,HTPB}}$ (2.4 J/gK) is taken from Veals et al. [29] Both $c_{\mathrm{p,HTPB}}$ and Q_d may be influenced by the addition of PMMA, which, however, would not significantly affect the model, as revealed by the sensitivity analysis in Fig. S1. Regression front temperature (T_r ~ 450 °C) is taken from the aforementioned TGA/DSC experiments [26,27], where the most significant weight loss of HTPB occurs at ~ 450 °C and can be regarded as the characteristic temperature on the surface. T_r will be further validated by our IR camera experiments, as discussed in Section 4.2.

4. Results and discussion

4.1. Manipulating the regression rate of HTPB by laser heating

Fig. 4 shows the measured HTPB regression rate under different laser intensity conditions. A total of five laser energy densities are studied not including $I_{\mathrm{L}} = 0$ as the base case.

It is quite clear that the regression rate of HTPB is very sensitive to laser input. Compared to the reference condition where regression rate is ~ 0.18 mm/s, the regression rate at the highest laser energy density (14 W/cm^2) is ~ 0.31 mm/s, showing an enhancement of roughly 72 % and can be readily and rapidly manipulated by adjusting the laser energy input. Meanwhile, to achieve a significant enhancement in regression rate, the upstream delivery method requires less laser energy than the downstream delivery methods reported in previous studies [13,25].

Model prediction results are also presented in Fig. 3. The relationship between the measured regression rate and laser energy density is close to linear, which implies that energy-balance model discussed in Section 3 can quantitively describe the regression of solid fuel with the laser heating. When the absorption efficiency η is set as 40 % (i.e., 60 % of laser energy penetrates through the decomposition zone), the model shows good agreement with the experimental results. A simple validation experiment is also conducted as follows: a high-speed airflow is used to extinguish the flame during the HTPB regression, and the transmitted laser energy above the burned surface I_{B} is measured using the previously described power meter. The absorption efficiency is then estimated by $\eta = 1 - I_{\mathrm{B}}/I_{\mathrm{L}}$. The measured η ranges from 43 % to 60 %, similar to the assumed value used in the model.

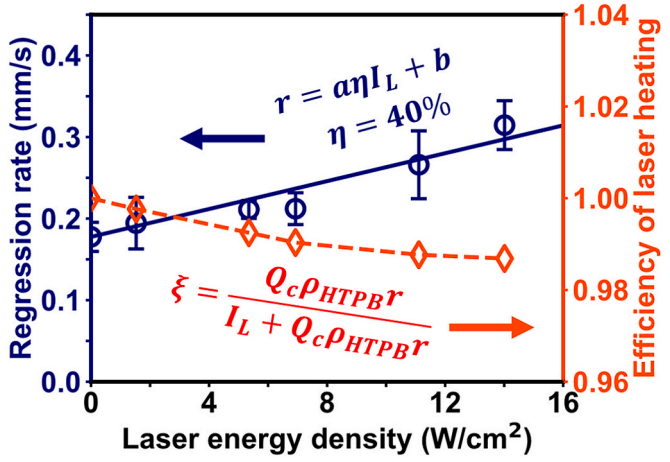

Fig. 4. Regression rates and efficiencies of laser heating of HTPB fuel at different laser energy densities. Dark blue symbols are the experimental results on regression rate. Dark blue line is the regression rate predicted by energy-balance model. Orange symbols are the efficiencies calculated by Eq. (6) while orange line is drawn to guide the eye.

Since the laser provides the additional heat to promote combustion, we estimate the energy penalty of the laser input relative to the gained power. Eq. (6) defines the efficiency of laser heating as the ratio of the combustion heat generation to the sum of laser energy input I_L (W/cm^2) and combustion heat generation.

$$\xi = \frac{Q_c \rho_{HTPB} r}{I_L + Q_c \rho_{HTPB} r} \tag{6}$$

If we assume that HTPB is fully oxidized, and its heat of combustion is Q_c ~ 38 kJ/g [30]. The efficiency of laser heating , as calculated from Eq. (6) is also presented in Fig. 4. ξ is seen to decrease monotonically with increasing laser energy flux. Nevertheless, in the investigated laser energy density range, the energy penalty is negligible ($\xi \rightarrow 1$). In other words, the energy generated by combustion is significantly larger than the energy delivered by the laser, which ensures the feasibility of the strategy of manipulating regression rate by laser heating. However, it should be highlighted that the actual efficiency of the system in practical applications will be influenced by various factors such as laser wall-plug efficiency and incomplete combustion.

The reason why laser heating can so effectively manipulate regression rate even though the delivered energy is much less than the combustion heat generation, is revealed by the comparison between I_{L} and $H_{\mathrm{F,1}}$. According to Eq. (3), $H_{\mathrm{F,1}}$ contributes to the regression rate in the absence of a laser, while I_{L} contributes to the increase of regression rate when laser energy input increases. It can be noticed that I_{L} and $H_{\mathrm{F,1}}$ are actually of the same magnitude, which can also be supported by the phenomenon that HTPB undergoes decomposition solely due to the laser energy input, without ignition, as presented by Fig. S2. This is because the majority of the combustion energy release is convected away for the fuel surface due to thermally driven gas-expansion. Therefore, the heat feedback to the regression front ($H_{\mathrm{F,1}}$) is poor, restricting flame propagation. In contrast, the laser energy is deposited directly to the regression front, providing localized and targeted heating, overcoming the natural convective heat loss and insufficient heat feedback. As a result, even modest levels of laser power can lead to substantial enhancement on fuel regression rate.

In addition to the regression rate, the influence of laser-regression front coupling on surface temperature of HTPB fuel is also of interest. Fig. 5 (a) and (b) shows representative infrared images of the regression front of HTPB with PMMA fiber without laser and at 11.1 W/cm^2 respectively. We find that the average temperature of the regression front is ~ 450 °C, regardless of laser input. Previous studies demonstrated that the dependency of thermal decomposition temperature of HTPB on heating rate is low; for instance, TGA experiments by Du [31] showed that increasing heat rate from 8 K/min to 60 K/min only changes the temperature of HTPB decomposition by ~ 30 °C. Previous studies across different experimental conditions also reported a similar second-stage decomposition temperature at ~ 450 °C [19,20,26]. In other words, the decomposition temperature of HTPB can be regarded as its inherent chemical property; additional energy from laser can only accelerate its decomposition, but cannot change its decomposition temperature significantly. The constant surface temperature observed by the IR camera also demonstrates that T_r ~ 450 °C in our model is a good approximation (as discussed in Section 3).

Similar phenomenon was also described in the work by Kakami et al. [12], where laser energy was delivered from the downstream and the surface temperature of fuel was constantly ~ 450 °C, independent of laser intensities.

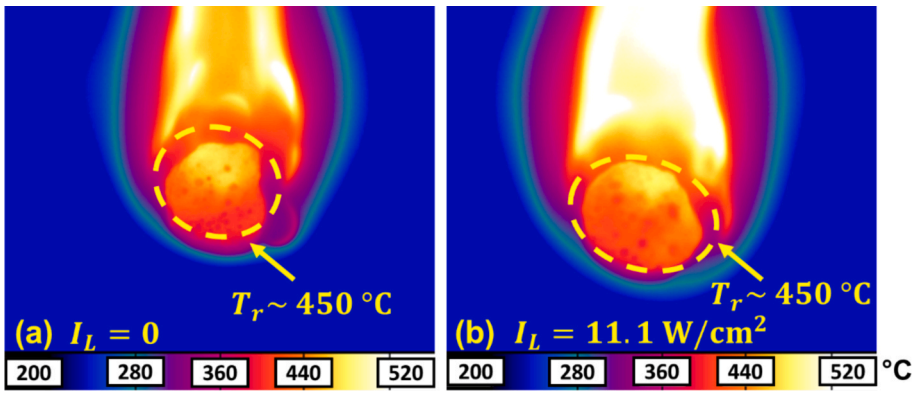

Fig. 5. IR images of the regression front without laser energy input (a) and with laser energy input (b), showing that surface temperature is unaffected by laser.

4.2. *Influence of additives*

We have demonstrated that employing a PMMA optical fiber to couple laser energy input and the regression front is an effective method for the manipulation of solid fuel combustion in the last section. According to the energy-balance model, despite a relatively low laser absorption efficiency of 40 %, the regression rate of HTPB exhibits a marked enhancement. Therefore, one can expect considerable potential for further improvement. In this section, we explore the incorporation of selected additives to enhance laser absorption, with the aim of achieving a more effective manipulation of regression rate.

Fig. 6(a-c) shows the dependence of regression rate on laser energy density for HTPB fuel with different additives. The weight percentages of graphite flakes and Al nanoparticles are 1 % and 5 % respectively. Higher graphite loadings are not selected due to the risk of premature ignition, likely caused by the excessive laser energy absorption of the unburned zone.

In the absence of any laser input, the regression rates of HTPB with different additives are all very similar. HTPB/graphite shows a slightly lower regression rate compared to HTPB and HTPB/nAl probably because of the lower oxidation reactivity of graphite.

When the laser energy is delivered, the regression rate of HTPB fuel doped with graphite shows the most significant dependence of laser intensity. As laser energy density increases to 0 and 11.1 W/cm^2, the regression rate of HTPB/Graphite increases significantly from ~ 0.16 mm/s to ~ 0.32 mm/s, showing an enhancement of roughly 100 %. It demonstrates that the incorporation of graphite further enhances the increasing of regression rate by laser heating, owing to its excellent optical absorption, which facilitates more efficient energy transfer from light to heat in the regression front. In contrast, the incorporation of Al nanoparticles does not improve the laser-induced enhancement effect. As laser energy density increases to 0 and 11.1 W/cm^2, the regression rate of HTPB/nAl increased from ~ 0.18 mm/s to ~ 0.26 mm/s, showing a similar enhancement effect compared to HTPB. Unlike graphite, Al has a higher reflectivity in the visible and thus does not couple well with the laser.

Fig. 6(d) presents the slopes of the regression rate – laser energy density relationship for HTPB with additives, and it is clear that HTPB/Graphite shows the most promoting effect, although its additive concentration is lower than that of HTPB/nAl.

5. Conclusions

A novel method is proposed to couple light into the regression front of solid fuels by embedding a high-efficiency fuel-based light pipe (PMMA) within HTPB. In this way the PMMA acts both as a laser energy conduit as well as a polymer fuel. The use of this approach mitigates many of the practical problems of coupling radiation energy to the regression front.

Experimental result demonstrates this concept. With laser energy

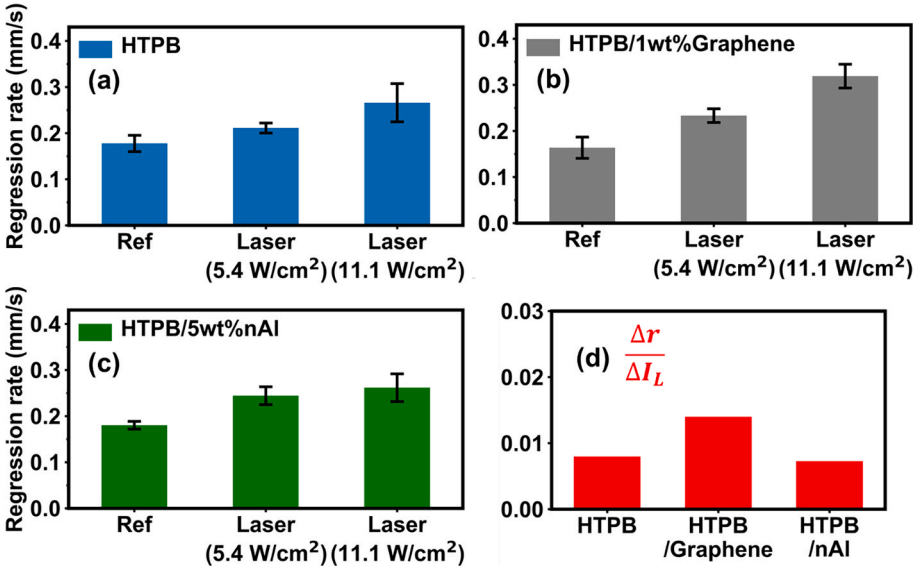

Fig. 6. Regression rate vs. Laser intensity for (a) HTPB fuel, (b) HTPB fuel doped with graphite flakes (1 wt%) and (c) HTPB fuel doped with Al nanoparticles (5 wt %); (d) the dependence of regression rate on laser intensity for HTPB with different additives.

input, the regression rate of HTPB can be enhanced significantly; from ~ 0.18 mm/s to ~ 0.31 mm/s as laser energy density increases from 0 to 14 W/cm^2. When HTPB is doped with graphite, the enhancement effect of laser heating can even be improved, as the graphite in the regression front can absorb laser irradiation better than HTPB and its decomposition products.

A one-dimensional energy-balance model shows that the energy penalty of using a laser to the energy output is less than 2 %, even at the highest laser energy used. Both experimental and computational results indicate that the dependency of regression rate on laser energy density is close to linear, offering a good strategy to manipulate regression rate.

CRediT authorship contribution statement

Yuxin Zhou: Writing – original draft, Methodology, Investigation, Formal analysis, Data curation. **Lei Yang:** Data curation. **Keren Shi:** Data curation. **Michael R Zachariah:** Writing – review & editing, Resources, Methodology, Investigation, Funding acquisition.

Declaration of competing interest

The authors declare that they have no known competing financial interests or personal relationships that could have appeared to influence the work reported in this paper.

Acknowledgements

The authors thank the support from ONR.

Appendix A. Supplementary data

Supplementary data to this article can be found online at https://doi.org/10.1016/j.fuel.2025.136476.

Data availability

Data will be made available on request.

References

[1] Zarko V, Kiskin A, Cheremisin A. Contemporary methods to measure regression rate of energetic materials: a review. Prog. Energy Combust. Sci. 2022;91:100980. https://doi.org/10.1016/j.pecs.2021.100980.
[2] Bidwai S, Welch MA, Michael JB, Young G. Temperature measurement of solid fuel polyoxymethylene counterflow diffusion flames using hybrid fs/ps CARS. AIAA SCITECH 2024 Forum, American Institute of Aeronautics and Astronautics. DOI: 10.2514/6.2024-1924.
[3] Geipel CM, Bojko BT, Pfützner CJ, Fisher BT, Johnson RF. Regression of solid polymer fuel strands in opposed-flow combustion with gaseous oxidizer. Proc. Combust. Inst. 2023;39:3389–99. https://doi.org/10.1016/j.proci.2022.07.124.
[4] Young G, Risha G, Miller AG, Glass RA, Terrence L. Connell J, Yetter RA. COMBUSTION OF ALANE-BASED SOLID FUELS. International Journal of Energetic Materials and Chemical Propulsion 2010; 9. DOI: 10.1615/IntJEnergeticMaterialsChemProp.v9.i3.50.
[5] Zhou Y, Zachariah MR. Computational Study on the Lifting of Aluminum Particles from a Hydroxyl-Terminated Polybutadiene burning Surface. J. Phys. Chem. C 2025;129:5696–701. https://doi.org/10.1021/acs.jpcc.4c08542.
[6] Wang H, Hagen E, Shi K, Herrera S, Xu F, Zachariah MR. Carbon fibers as additives to engineer agglomeration and propagation of aluminized propellants. Chem. Eng. J. 2023;460:141653. https://doi.org/10.1016/j.cej.2023.141653.
[7] Zhou Y, Zachariah MR. Molecular Dynamics Study on the Capture of Aluminum Particles by Carbon Fibers during the Propagation of Aluminum-based Energetics. Energy Fuels 2024;38:8992–9000. https://doi.org/10.1021/acs.energyfuels.4c00832.
[8] Wang Y, Chowdhury M, Zhou Y, Issac Paul G, Shi K, Zachariah MR. Oscillating-to-Continuous Combustion transition in Mesoparticle Composites through Manipulation of Heat Feedback. Adv. Funct. Mater. 2024;34:2406722. https://doi.org/10.1002/adfm.202406722.
[9] Shi K, Wang Y, Zachariah MR. Microwave antenna focusing for spatially resolved modulation of burn rate. Chem. Eng. J. 2024;492:152192. https://doi.org/10.1016/j.cej.2024.152192.
[10] Shi K, Bokhoor M, Wang Y, Weihs TP, Zachariah MR. Propagation rate and product modulation in SHS reactions via focused microwave heating. Chem. Eng. Sci. 2025;302:120794. https://doi.org/10.1016/j.ces.2024.120794.
[11] Barkley SJ, Zhu K, Lynch JE, Michael JB, Sippel TR. Microwave plasma enhancement of multiphase flames: On-demand control of solid propellant burning rate. Combust. Flame 2019;199:14–23. https://doi.org/10.1016/j.combustflame.2018.10.007.
[12] Kakami A, Hiyamizu R, Shuzenji K, Tachibana T. Laser-Assisted Combustion of Solid Propellants at Low pressures. J. Propul. Power 2008;24:1355–60. https://doi.org/10.2514/1.36458.
[13] Duan B, Zhang H, Hua Z, Wu L, Bao Z, Guo N, et al. Burning characteristics and combustion wave model of AP/AN-based laser-controlled solid propellant. Energy 2022;253:124007. https://doi.org/10.1016/j.energy.2022.124007.
[14] Esker DR, Brewster MQ. Laser pyrolysis of hydroxyl-terminated polybutadiene. J. Propul. Power 1996;12:296–301. https://doi.org/10.2514/3.24027.
[15] Uhlenhake KE, Gomez M, Collard DN, Örnek M, Son SF. Laser ignition of solid propellants using energetic nAl-PVDF optical sensitizers. Combust. Flame 2023;254:112848. https://doi.org/10.1016/j.combustflame.2023.112848.
[16] Collard DN, Uhlenhake KE, Örnek M, Rhoads JF, Son SF. Photoflash and laser ignition of Al/PVDF films and additively manufactured igniters for solid propellant. Combust. Flame 2022;244:112252. https://doi.org/10.1016/j.combustflame.2022.112252.
[17] Quagliano Amado JC, Ross PG, Mattos Silva Murakami L, Narciso Dutra JC. Properties of Hydroxyl-Terminal Polybutadiene (HTPB) and its use as a Liner and Binder for Composite Propellants: a Review of recent advances. Propellants Explos. Pyrotech. 2022;47:e202100283. https://doi.org/10.1002/prep.202100283.
[18] Dennis C, Bojko B. On the combustion of heterogeneous AP/HTPB composite propellants: a review. Fuel 2019;254:115646. https://doi.org/10.1016/j.fuel.2019.115646.
[19] Mahottamananda SN, Pal Y, Yadav N, Trache D, Tarchoun AF, Abdelaziz A, et al. Combustion of HTPB-based solid fuels containing Viton-coated Boron for hybrid rocket applications. FirePhysChem 2024. https://doi.org/10.1016/j.fpc.2024.12.004.
[20] Jouini M, Abdelaziz A, Trache D, Tarchoun AF, Amokrane S, Benzetta A, et al. HTPB propellant binder supplemented with nitro potato starch: Formulation, characterization, and thermal decomposition behavior. FirePhysChem 2024;4:211–5. https://doi.org/10.1016/j.fpc.2023.11.003.
[21] Qian Y, Wang Z, Chen L, Liu P, Jia L, Dong B, et al. A study on the decomposition pathways of HTPB and HTPE pyrolysis by mass spectrometric analysis. J. Anal. Appl. Pyrol. 2023;170:105929. https://doi.org/10.1016/j.jaap.2023.105929.
[22] Huang C-W, Huang P-H, Yang Z-Y, Li Y-H. A study on iron-composite polymer propellants for improved plasma generation in electric propulsion systems. Chem. Eng. J. 2025;508:160990. https://doi.org/10.1016/j.cej.2025.160990.
[23] Singh AV, Gollner MJ. Steady and transient pyrolysis of a non-charring solid fuel under forced flow. Proc. Combust. Inst. 2017;36:3157–65. https://doi.org/10.1016/j.proci.2016.07.043.
[24] Lv X, Zha M, Ma Z, Zhao F, Xu S, Xu H. Fabrication, Characterization, and Combustion Performance of Al/HTPB Composite Particles. Combust. Sci. Technol. 2017;189:312–21. https://doi.org/10.1080/00102202.2016.1210604.
[25] Kakami A, Tachibana T. Heat balance evaluation of double-base solid propellant combustion using thermography and laser heating on a burning surface. Aerosp. Sci. Technol. 2015;47:86–91. https://doi.org/10.1016/j.ast.2015.09.013.
[26] Chen JK, Brill TB. Chemistry and kinetics of hydroxyl-terminated polybutadiene (HTPB) and diisocyanate-HTPB polymers during slow decomposition and combustion-like conditions. Combust. Flame 1991;87:217–32. https://doi.org/10.1016/0010-2180(91)90109-O.
[27] Lu Y-C, Kuo KK. Thermal decomposition study of hydroxyl-terminated polybutadiene (HTPB) solid fuel. Thermochim Acta 1996;275:181–91. https://doi.org/10.1016/0040-6031(95)02726-2.
[28] DeLuca LT, Galfetti L, Maggi F, Colombo G, Merotto L, Boiocchi M, et al. Characterization of HTPB-based solid fuel formulations: Performance, mechanical properties, and pollution. Acta Astronaut. 2013;92:150–62. https://doi.org/10.1016/j.actaastro.2012.05.002.
[29] Veals J, Chen C-C, Yeh I-C, Stone C, McQuaid M. Property estimates for Hydroxyl-Terminated Polybutadiene (HTPB) Type R45M Derived from Atomistic Molecular Dynamics Simulations. Aberdeen Proving Ground, MD: DEVCOM Army Research. Laboratory 2023. https://doi.org/10.21236/AD1204916.
[30] Sinha YK, Sridhar BTN, Kishnakumar R. Study of Thermo-Mechanical Properties of HTPB–Paraffin Solid fuel. Arabian Journal of Science and Engineering 2016;41:4683–90. https://doi.org/10.1007/s13369-016-2230-3.
[31] Tingfa D. Thermal decomposition studies of solid propellant binder HTPB. Thermochim Acta 1989;138:189–97. https://doi.org/10.1016/0040-6031(89)87255-7.